

Constraining cosmic curvature by using age of galaxies and gravitational lenses

Akshay Rana,^{a,1} Deepak Jain,^b Shobhit Mahajan,^a Amitabha Mukherjee^a

^aDepartment of Physics and Astrophysics, University of Delhi, Delhi 110007, India

^bDeen Dayal Upadhyaya College, University of Delhi, Sector-3, Dwarka, Delhi 110078, India

E-mail: arana@physics.du.ac.in, djain@ddu.du.ac.in, shobhit.mahajan@gmail.com, amimukh@gmail.com

Abstract. We use two model-independent methods to constrain the curvature of the universe. In the first method, we study the evolution of the curvature parameter (Ω_k^0) with redshift by using the observations of the Hubble parameter and transverse comoving distances obtained from the age of galaxies. Secondly, we also use an indirect method based on the mean image separation statistics of gravitationally lensed quasars. The basis of this methodology is that the average image separation of lensed images will show a positive, negative or zero correlation with the source redshift in a closed, open or flat universe respectively. In order to smoothen the datasets used in both the methods, we use a non-parametric method namely, Gaussian Process (GP). Finally from first method we obtain $\Omega_k^0 = 0.025 \pm 0.57$ for a presumed flat universe while the cosmic curvature remains constant throughout the redshift region $0 < z < 1.37$ which indicates that the universe may be homogeneous. Moreover, the combined result from both the methods suggests that the universe is marginally closed. However, a flat universe can be incorporated at 3σ level.

Keywords: Curvature density, Age of galaxy, Gravitational Lensing, Image separation, Gaussian process.

¹Corresponding author.

Contents

1	Introduction	1
2	Method I : Null test of cosmic curvature using $H(z)$ and age of galaxies	2
2.1	Estimating the transverse comoving distance using the age-redshift dataset of galaxies	2
2.2	Hubble dataset	3
2.3	Methodology	5
3	Method II : Constraining cosmic curvature using the mean image separation of gravitational lenses	5
3.1	Dataset and methodology	7
4	Results and Discussions	9
4.1	Method I	9
4.2	Method II	10

1 Introduction

Cosmic curvature is a fundamental parameter in cosmology. It plays a crucial role in the evolution of universe. Furthermore, the combined observational constraints by SNe Ia, BAO, Hubble Data and WMAP survey also suggest that Ω_k^0 is indeed very small [1]. Recently, Planck survey has given very precise bounds on curvature density, $\Omega_k^0 = 0.000 \pm 0.005$ (95%, Planck TT+lowP+lensing+BAO) [2]. Interestingly, in order to find the solution of cosmological constant and coincidence problem, Shaw & Barrow [3] also predicted the spatial curvature parameter $\Omega_k^0 = -0.0055$ which is also consistent with Planck result. Though the flatness of universe obtained from the cosmological observations is almost at an unprecedented level of precision, its interpretation still depends on the fact that the background cosmology is described by homogeneous and isotropic FLRW metric. In order to test the FLRW metric and curvature of the universe, Clarkson et. al. proposed that any detection of redshift dependence of curvature parameter would imply presence of non FLRW cosmology [4].

Another important issue is the presence of the geometric degeneracy between dark energy equation of state parameter $w(z)$ and cosmic curvature Ω_k^0 . This degeneracy prevents us from understanding the nature of dark energy. To circumvent this problem, most of the work neglects Ω_k^0 (by advocating that several observations put very small bounds on Ω_k^0) and attempts to find bounds on $w(z)$ independently. However, it has been found that ignoring Ω_k^0 leads to errors in the reconstruction of $w(z)$ and even a small value of Ω_k^0 induces a large effect at higher redshifts $z \simeq 1$ and the inclusion of cosmic curvature in the analysis offers a wide range of dark energy models which can explain the accelerating universe. [5–8]. Hence it seems inconsistent to neglect the contribution of Ω_k^0 , howsoever small it might be. [9]. Moreover many dark energy tests such as the Integrated Sachs-Wolfe (ISW) effect and cluster surveys are also very sensitive to the assumption about Ω_k^0 [10]. In addition, weak lensing and baryon acoustic oscillation (BAO) datasets have also been used to constrain the cosmic curvature based on the distance sum rule [11, 12]. However, the efficiency of this test is limited because of the large uncertainties in the weak gravitational lensing datasets. Many alternate theories (theories based on the anthropic principle [13], the Inhomogeneous universe [14] and the Irrotational dust universe [15] etc.) have been proposed to address the fine tuning of parameters and the presence

of dark energy. Furthermore, a precise measure of cosmic curvature can act as an excellent test for several inflationary models of the universe supporting flat [16–18] or open universe [19–26]. Hence it is very important to constrain Ω_k^0 in a model independent manner.

In this paper, we use two different model independent techniques to estimate the curvature of the universe. In Method I, we determine Ω_k^0 by using the independent dataset of Hubble parameter $H(z)$ and the transverse comoving distance obtained by using the age of galaxies [27]. A prominent feature of this analysis is that it doesn't rely on any assumption of the underlying cosmological model. If we find any deviation in the evolution of cosmic curvature then it is an indication of new physics. We apply Gaussian Process (GP) smoothing technique to the data points to infer any violation of FLRW based cosmological models. In Method II, Ω_k^0 is constrained by using the statistical properties of gravitational lens systems. Gott, Park and Lee showed that for the Singular Isothermal Spherical (SIS) model of galaxies, the mean image separation $\langle \Delta\theta \rangle$ is independent of the source redshift if the universe is assumed to be flat in FLRW universe [28]. We use an updated dataset of 44 gravitational lenses from the DR7 SDSS gravitational lens dataset [29]. We again apply the non-parametric technique of Gaussian Process on the image separation data points to constrain the cosmic curvature.

The structure of the paper is as follows: In Section 2, we discuss Method I based on the determination of the cosmic curvature in a model independent manner and methodology to obtain the transverse comoving distance from the age of galaxies. In Section 3, we explain Method II which is based on the image separation statistics of gravitationally lensed quasars. We analyze the results in Section 4.

2 Method I : Null test of cosmic curvature using $H(z)$ and age of galaxies

This method provides a model independent test of spatial curvature of the universe. It is based on a geometrical relation between the Hubble parameter $H(z)$, transverse comoving distance $r(z)$ and its first derivative $r'(z)$. It enable us to check whether the present curvature density is independent of the redshift of measurement or not. This test was firstly proposed by Clarkson et.al. [4] and further used by several authors [30–36] where independent observations of Hubble parameter and transverse comoving distances are used to constrain the cosmic curvature. The relation is given as ;

$$\Omega_k^0 = \frac{H(z)^2 r'(z)^2 - c^2}{H_0^2 r(z)^2} \quad (2.1)$$

It measure the present curvature density by using the independent observations of $H(z)$ and transverse comoving distance at one single redshift. In any FLRW universe, the curvature parameter remains independent of redshift of measurement. In other words, If the present curvature parameter is found to be dependent on the redshift of measurement, then there is a need to explore the models beyond FLRW metric. Eq.2.1 provide us the simplest way to analyze the present cosmic curvature by using the independent measurements of $H(z)$, $r(z)$ and $r'(z)$ at a given redshift.

2.1 Estimating the transverse comoving distance using the age-redshift dataset of galaxies

To find the transverse comoving distance $r(z)$ and its derivative $r'(z)$, we use 32 data points of age of galaxy ($0.11 < z < 1.84$) plus one data point from the Planck survey for the present age of the universe. Out of these 32 data-points, 20 are red galaxies from the Gemini Deep Survey (GDDS)[37], 10 are early field type galaxies [38] whose ages are obtained by using SPEED models [39] and there are two radio galaxies LBDS 53W069 and LBDS 53W091 [40].

The transverse comoving distance $r(z)$ can be obtained from the age-redshift data of galaxies [27]. FLRW cosmology enables us to write down the transverse comoving distance $r(z)$ in the form of the first derivative of the age of the galaxy,

$$r(z) = \begin{cases} \frac{c}{H_0 \sqrt{|\Omega_k^0|}} \sinh [H_0 \sqrt{|\Omega_k^0|} \int_z^0 (1 + \dot{z}) \frac{dt}{dz} dz] & \text{for } \Omega_k^0 > 0 \\ c \int_z^0 (1 + \dot{z}) \frac{dt}{dz} dz & \text{for } \Omega_k^0 = 0 \\ \frac{c}{H_0 \sqrt{|\Omega_k^0|}} \sin [H_0 \sqrt{|\Omega_k^0|} \int_z^0 (1 + \dot{z}) \frac{dt}{dz} dz] & \text{for } \Omega_k^0 < 0 \end{cases} \quad (2.2)$$

where t is the age of universe at redshift z . If one can determine $\frac{dt}{dz}$ at the required redshift then one can easily reconstruct the value of transverse comoving distance $r(z)$. For this purpose we use an age-redshift dataset of 32 old, passive galaxies distributed over the redshift interval of $0.11 < z < 1.84$. Further we add an incubation time $t_{inc} = 1.50 \pm 0.45$ Gyr that accounts for the time from the beginning of the universe to the formation of the first galaxy. This is the mean value of the incubation bound obtained by Wei et. al. [41] using the age of a galaxy sample in a flat Λ CDM model. However, a 12% error is given in the analysis of measurement of age of galaxies which we take as the uncertainty in measurement [42–44].

The present age of universe is taken to be 13.790 ± 0.021 Gyr obtained by Planck survey with a joint analysis of CMB + BAO + SNe Ia + H_0 [2]. Once we have the dataset, we fit this data using a third degree polynomial $t(z) = A + Bz + Cz^2$. The best fit values turn out to be (in Gyr): $A = 13.78 \pm 0.01$, $B = -10.65 \pm 0.84$, $C = 2.98 \pm 0.34$ with a $\chi^2_\nu = 0.41$. The best fit curve is shown in Fig. 1.

On differentiating the polynomial, we obtain $\frac{dt}{dz} = B + 2Cz$. Now here we choose $\Omega_k^0 = 0$ and by using Eq. 2.2, we obtained the transverse comoving distance;

$$r(z) = c \left[-B \left(z + \frac{z^2}{2} \right) - C \left(z^2 + \frac{2z^3}{3} \right) - D \left(z^3 + \frac{3z^4}{4} \right) \right] \quad (2.3)$$

and on further differentiating it, we get

$$r'(z) = c \left[-B (1 + z) - 2C (z + z^2) - 3D (z^2 + z^3) \right] \quad (2.4)$$

It is important to note that transverse comoving distance $r(z)$ also depends on the value of Ω_k^0 so it can be derived using different values of Ω_k^0 . However, our aim here is only to study the evolution of Ω_k^0 with redshift z . It helps to check the consistency of the FLRW metric as well as homogeneity of the universe. Therefore, any choice of Ω_k^0 to derive the transverse comoving distance would fulfill our purpose.

In order to check the variation of Ω_k^0 by using the observations at different redshift, we further need the Hubble data along with transverse comoving distance $r(z)$ and its first derivative $r'(z)$.

2.2 Hubble dataset

We use a recent dataset of $H(z)$ consisting of 38 data points which are derived using various observational methods and datasets [see Table 3]. It is important to stress that in order to derive the value of

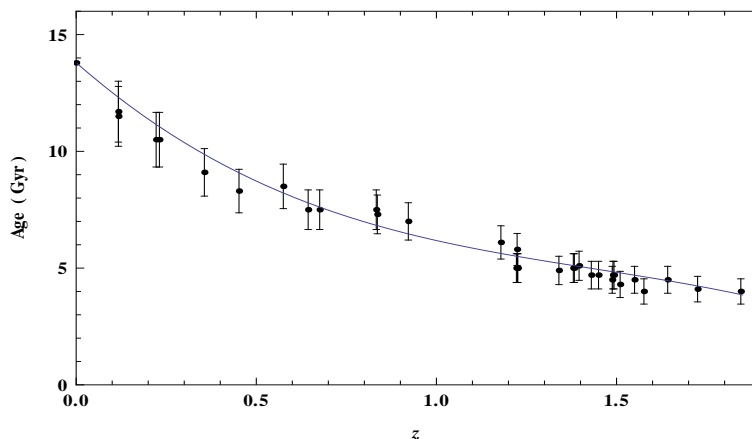


Figure 1: Age of galaxy $t(z)$ vs z . The black points are the original data of 32 points added with an incubation time $t_{inc} = 1.50 \pm 0.45$ Gyr. The blue line is obtained from the fit by using a third degree polynomial.

Ω_k^0 , both the datasets (i.e. $H(z)$ and age of galaxies used to calculate transverse comoving distances) must be independent of each other. Therefore we use the following methodology.

- It is observed that in the Hubble data set, 9 data-points are obtained by using the same 32 age of galaxy data points or their subsamples, which are used to derive the transverse comoving distances in our work [40]. So we remove these nine points from the Hubble dataset. These points are indicated by R^a in Table 3.

- Further in the Hubble dataset, all 38 measurements of $H(z)$ are not completely independent. Three measurements taken from Blake et.al (2012) [45] (See S.No. 16, 22 ,25 in Table 3) are correlated with each other and three measurements taken from Alam et.al (2016) [46] (See S.No. 11, 20, 23 in Table 3) are also correlated. All these points are derived from the BAO measurement. However, Farooq et al (2016) [8] have recently observed that the inclusion of the off-diagonal elements of the correlation matrix of these $H(z)$ measurements will produce a small effect on the likelihood function used for the parameter estimation. Following the same reasoning, we therefore treat these observations as independent by neglecting the off diagonal terms of correlation matrix in our analysis.

- The upper limit of redshift in the age dataset is $z < 1.84$. Hence we restrict our analysis till the redshift $z = 1.84$ and we drop the three $H(z)$ observations at $z = 1.965$ from Moresco et. al (2015) [47], $z = 2.34$ from Delubac et.al (2015) [48] and $z = 2.36$ from Font-Ribera et.al. (2014)[49] from the $H(z)$ dataset.

Finally, we are left with 26 observations of $H(z)$. By using these two independent datasets, the Hubble parameter and the transverse comoving distances derived by using the age of galaxies, we reconstruct a dataset of the cosmic curvature Ω_k^0 . The corresponding error bars are derived by using the standard error propagation method.

$$\sigma_{\Omega_k^0}^2 = 4(\Omega_k^0)^2 \left[\left(\frac{\sigma_r}{r} \right)^2 + \left(\frac{\sigma_{H_0}}{H_0} \right)^2 \right] + 4 \left[(\Omega_k^0)^2 + \frac{c^2}{(H_0 r)^2} \right] \left[\left(\frac{\sigma_H}{H} \right)^2 + \left(\frac{\sigma_{r'}}{r'} \right)^2 \right] \quad (2.5)$$

where σ_r , $\sigma_{r'}$, σ_H and σ_{H_0} are the errors in the transverse comoving distance $r(z)$, its first derivative $r'(z)$, the Hubble parameter $H(z)$ and the present value of Hubble constant H_0 respectively.

The value of H_0 to be used in the analysis is another issue. Chen & Ratra 2011) [50] have obtained a value $H_0 = 68 \pm 2.8$ Km/sec/Mpc which is widely supported by global observations [51–55]. On the other hand, using SNe Ia data, Riess et. al [56] have found $H_0 = 73.24 \pm 1.74$ Km/sec/Mpc. We carry out our analysis using both these values of the Hubble constant.

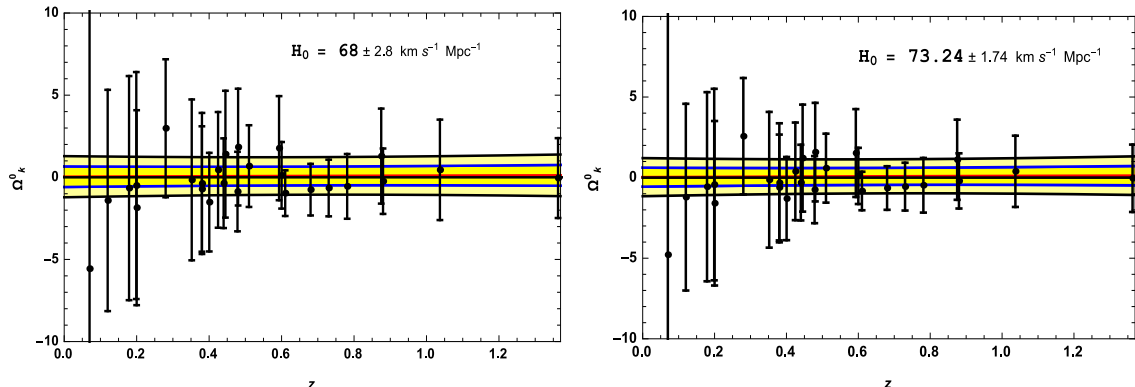


Figure 2: Smooth plots of Ω_k^0 vs z after applying Gaussian Process for different values of Hubble constant H_0 . The red line shows the best fit line while dark yellow and light yellow regions are the 1σ and 2σ confidence bands respectively. Black points are the 26 reconstructed datapoints of Ω_k^0 at different redshifts. The horizontal black line represents the $\Omega_k^0 = 0$ line.

2.3 Methodology

In order to understand the global behavior of Ω_k^0 , we employ a non-parametric method, namely Gaussian Process on the newly constructed dataset. It enables us to obtain a smoothed curve with the corresponding 1σ and 2σ confidence bands. In GP method, we presume that each observation is an outcome of an independent Gaussian distribution belonging to the same population. However the outcome of observations at any two redshifts are correlated due to their nearness to each other. This correlation between two points (say z & \hat{z}) is incorporated in the technique through a covariance function given by

$$k(z, \hat{z}) = \sigma_f^2 \exp \left[\frac{-(|z - \hat{z}|)^2}{2l^2} \right] \quad (2.6)$$

In this function, the two hyperparameters, the length-scale l and output variance σ_f , determine the length of the ‘wiggles’ in the smoothing function and average distance of function from its mean respectively. The values of these hyperparameters is calculated by maximizing the corresponding marginal log-likelihood probability function of the distribution. For details see Rasmussen et. al.(2006)[57] & Seikel et.al (2012) [58].

Finally, by applying the Gaussian process on the dataset of Ω_k^0 obtain the best fit curves along with the 1σ and 2σ error bars.[See Fig.2].

3 Method II : Constraining cosmic curvature using the mean image separation of gravitational lenses

Gravitational lensing is an important observational tool in cosmology. This has an advantage over the other cosmological tools as it relies on relatively well understood physics. Various aspects of the

gravitational lensing have been studied elaborately which helps us to understand the geometry and the constituents of the universe. In their seminal work, TOG (1984) [59] studied the statistical properties of gravitational lenses in order to understand the cosmological parameters and their evolution. One of the important aspects of the statistical properties is the relation between the average image separation and source redshift. In this work, we have exploited this relation to put constraints on the cosmic curvature. This analysis is based on a fact that *the mean image separation is completely independent of the source redshift for all the FLRW based cosmological models in a flat universe i.e. $\Omega_k = 0$, if the lensing galaxy is non-evolving and modelled as a Singular Isothermal Sphere (SIS).*[28, 60–64] In this case, the normalized mean image separation $\frac{\langle \Delta\theta(z_s) \rangle}{\Delta\theta_0}$ for the SIS galaxy lenses can be defined as [60–62]

$$\frac{\langle \Delta\theta(z_s) \rangle}{\Delta\theta_0} = \frac{\left(\int_0^{z_s} \frac{D_{LS}^3 D_{OL}^2 (1+z_L)^2}{D_{OS}^3 E(z_L)} dz_L \right)}{\left(\int_0^{z_s} \frac{D_{LS}^2 D_{OL}^2 (1+z_L)^2}{D_{OS}^2 E(z_L)} dz_L \right)} \quad (3.1)$$

where z_L & z_S are the lens and source redshifts respectively. L , S and O represent the lens, source and observer, while D_{LS} , D_{OL} & D_{OS} indicate the corresponding angular diameter distances between the lens, source and observer (for mathematical expressions see [65]). Further $E(z) = H(z)/H_0$ and $\Delta\theta_0 = \frac{8\pi\sigma_v^2}{c^2}$, where $H(z)$ is the Hubble parameter and σ_v is the velocity dispersion of the lens galaxy. [66].

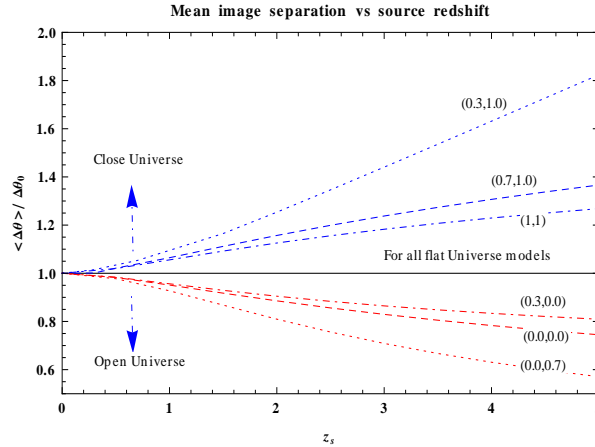


Figure 3: Normalized mean image separation $\frac{\langle \Delta\theta \rangle}{\Delta\theta_0}$ vs source redshift z_s for different cosmological models. Values in brackets represents the matter density and the cosmological constant density i.e. $(\Omega_m, \Omega_\Lambda)$ configurations, while the black solid line is for all possible flat universe configurations i.e. $\Omega_m + \Omega_\Lambda = 1$.

In Fig.3, we plot the normalized mean image separation $\frac{\langle \Delta\theta(z_s) \rangle}{\Delta\theta_0}$ vs source redshift z_s . It shows that for the SIS model of lenses the image separation integrated over the lens redshift $z_L = 0$ to $z_L = z_s$ is completely independent of the source redshift z_s for a flat universe. However, the mean image separation decreases with source redshift in an open universe and increases in a closed universe. In a closed universe the volume decreases faster with redshift than in a flat universe, and the source is more likely to be lensed by the lensing galaxies at shorter distances, which in turn produces large image separations, and vice versa for an open universe. The aim of this work is to

analyze the present available data for exploring the possible correlation between the average image separation and source redshift. Any correlation will shed some light on the cosmic curvature.

3.1 Dataset and methodology

We use the final statistical sample of lensed quasars from the Sloan Digital Sky Survey (SDSS) Quasar Lens Search (SQLS). This SDSS DR7 quasar catalog consists of a well-defined statistical lens sample of 26 lenses and 36 additional lenses identified with various techniques[29]. However as we are assuming the SIS model of galaxies for lenses, this limits the number of source images to two or a perfect Einstein ring. So we select only those lens systems which have two images. Since the image separations in some lens systems are too large which can not be explained comfortably by assuming the SIS lens model [61, 67]. Therefore we impose a selection criterion according to which the maximum image separation between two images should be less than $4''$ [68]. After applying these criteria on a dataset containing 62 lensing systems, we are finally left with 44 galaxy lenses only. For calculating the mean image separation first we divided this dataset in the redshift bin-size of 0.3 and 0.5 each and then determine the mean value of $\Delta\theta$ in each interval (See Fig.5 upper panel). The size of the redshift bins are selected in such a way that two or more than two points should lie in each interval. Though a large bin size will increase the bias in the result, we believe that with the availability of more data points in the near future may reduce the bias in the result.

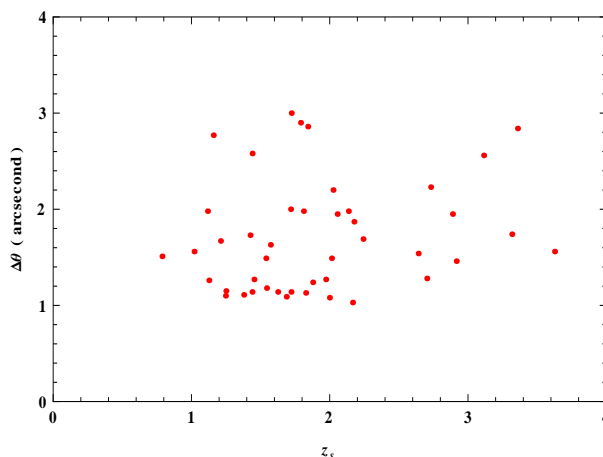


Figure 4: Observed data of statistical sample of lensed quasars from the Sloan Digital Sky Survey (SDSS) Quasar Lens Search (SQLS) (44 data points) after applying selection criteria.

In this method, our aim is to make use of the fact that the mean image separation of lensed sources remains constant with respect to the source redshift for all possible flat universe models, if the lensing galaxies follow the SIS model. This enables us to differentiate between an open, closed and flat universe. In our analysis, we use the image separation of 44 gravitational lenses and further created two datasets of 9 and 6 data points by assuming redshift bins of size 0.3 and 0.5 respectively. We apply the Gaussian process on these two datasets to study the variation of mean image separation with respect to source redshift. In the flat universe the reconstructed curves should remain independent of source redshift as shown in Fig.3 and the normalized value of the mean image separation must have a constant value equal to one. By analyzing Fig.5, we find that the reconstructed curves are showing a very weak inclination towards a closed universe. However within the 2σ confidence region, both curves partially include the $\frac{\Delta\theta(z_s)}{\Delta\theta_0} = 1$ line. Thus, we can argue that the best fit line seems

to indicate a closed universe but within the 3σ confidence region it will accommodate the possibility of a flat universe easily.

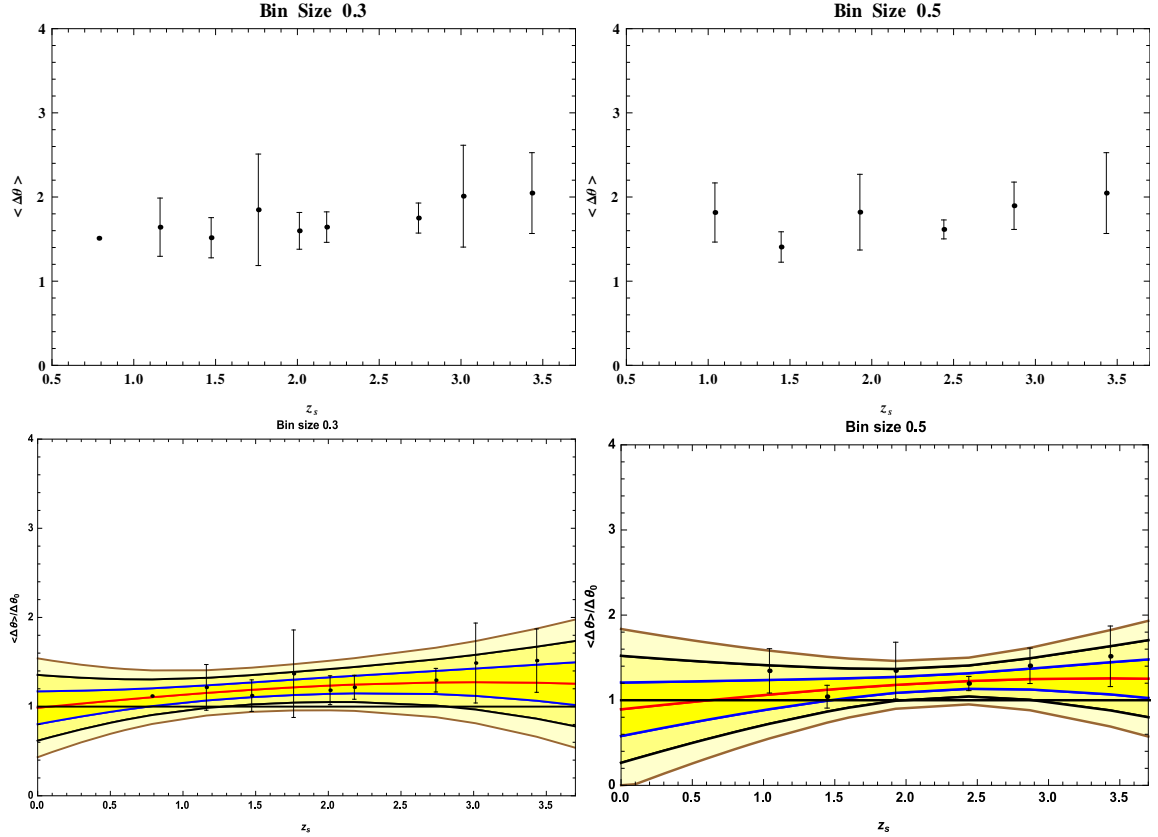


Figure 5: The upper two figures show the formation of different datasets using a binning size of 0.3 (upper left) and 0.5 (upper right) respectively. The lower panel of figures contains the smoothed curve of the normalized mean image separation datasets formed using a binning size 0.3 (left) and 0.5 (right) respectively. The red line shows the best fit line obtained using the Gaussian process with the 1σ , 2σ and 3σ confidence regions. While solid black line represent the theoretical variation of normalized mean image separation with source redshift z_s .

To further analyze this correlation between the image separation and the source redshift, we apply three statistical tests to check the correlation between parameters. Pearson product-moment correlation test, Spearman rank correlation test and Kendall rank correlation test are the well established tests which are widely used to check the linearity and monotonicity or in other words, the correlation between two parameters [69]. Out of these three tests, the Pearson product-moment correlation test gives a parametric measure of the degree of linear dependence between two variables and is denoted by the symbol r . The other two methods of Spearman’s rank correlation test and Kendall rank correlation test are a nonparametric measure of the strength and direction of association that exists between two variables or check their statistical dependence and are represented by ρ and τ respectively. The coefficient corresponding to each test takes a range of values from $+1$ to -1 . A value of zero indicates that there is no correlation between the two variables. A value greater and smaller than zero indicates a positive and negative correlation respectively. The value of r , ρ and τ with the corresponding error bars are mentioned in the Table 1. Each statistical test indicates a weak positive correlation between image separation $\Delta\theta$ and source redshift z_s . These tests also shows their

Statistical tests	value
Spearman's rank coefficient (ρ)	0.22 ± 0.09
Pearson product-moment coefficient (r)	0.20 ± 0.15
Kendall rank correlation coefficient (τ)	0.13 ± 0.01

Table 1: Statistical tests to check the correlation between image separation and source redshift.

consistency with the variation of reconstructed curve shown in Fig.5.

4 Results and Discussions

Given the crucial role played by Cosmic curvature in the evolution of the universe, it is important to study the cosmic curvature in a model independent manner. Several methods have been proposed to determine the curvature parameter using different techniques. In this paper, we work with two different approaches. Method I is a Null test of cosmic curvature implemented by using a dataset of the Hubble parameter $H(z)$ and age of galaxies. In this approach, our main focus is to check the assumption of homogeneity and FLRW metric of the universe. On the other hand, Method II is based on the statistical properties of gravitational lenses. It gives us an indirect window to check the flatness of the universe if FLRW metric of the universe holds. Hence the outcome of Method I paves the way for Method II. In totality, it gives a measure of the consistency of flat universe based on FLRW metric. Here we will discuss the outcome of both the methods separately.

4.1 Method I

This technique is based on a model independent null test of cosmic curvature [4]. This test is presented as a test of homogeneity of universe. It highlights the importance of measuring the cosmic curvature in a more precise manner. The main logic behind the null test of curvature is the fact that if we have two mutually independent datasets of the Hubble parameter $H(z)$ and the transverse comoving distance simultaneously, then we can reconstruct the present value of the cosmic curvature at each redshift of measurement. In a FLRW universe Ω_k^0 should not depend on the redshift and if we observe any deviation from this, then it is a direct indication of deviation from a FLRW universe or a violation of the assumption of homogeneity of the universe [30, 70]. Efforts have been made to relate a violation of this null test of cosmic curvature to the inhomogeneous cosmology model [71]. Further Boehm et.al (2013) have presented the violation of this null test of curvature as a signature of back-reaction toy model with realistic features and have tried to confront it with the Union2.1 supernova data [72].

The prime challenge is to check the efficiency of this null test in a precise manner. Earlier Union2.0 SNe Ia dataset was used for calculating the transverse comoving distance and the Hubble parameter data points are obtained from differential ages of galaxies and radial BAO measurements[32, 73]. This method is termed as the differential approach for constraining cosmic curvature [31]. Sapone et.al (2014) test the efficiency of the method with four different statistical methods [30], while Yu et.al [74] test the cosmic curvature by comparing the proper distance and transverse comoving distance. Many combinations of observational datasets have been applied on this null test but all the combinations demonstrate their consistency with the FLRW universe and even support the flatness of universe within different confidence regions [33–35]. Though many efforts have been made to measure Ω_k^0 using various observational datasets, there is always a need to use a model independent

H_0 (Km/sec/Mpc)	Ω_k^0
68 ± 2.8	0.036 ± 0.62
73.24 ± 1.74	0.025 ± 0.57

Table 2: Best fit value of Ω_k^0 for different values of H_0

dataset. In earlier works transverse comoving distances were frequently obtained by using the SNe Ia dataset. This is matter of debate since calculation of distance modulus of SNeIa itself depends upon the dark energy model and also infected with systematic errors like cosmic opacity. However in this work we obtain the transverse comoving distance r using the age of galaxies [27] and combine it with the selected Hubble data points(see Table 3) to obtain a model independent bound on the cosmic curvature Ω_k^0 at different redshifts.

Our approach is completely model independent because the measurement of ages of old passively evolving galaxies relies only the detailed shape of the galaxy spectra but not on the galaxy luminosity [75]. Further to study the global behavior and to constrain the Ω_k^0 we apply a non parametric technique Gaussian Process and obtain a smoothened curve for it as shown in Fig.2. By analyzing this smoothened curve, we conclude that:

- The cosmic curvature in the redshift range $0 < z < 1.37$ remains constant with respect to redshift for both the values of H_0 used in this work. This further support a homogeneous FLRW universe. We can also infer that this null test disallows the possibility of an inhomogeneous universe. We calculate the best fit bounds on Ω_k^0 using different values of H_0 for a presumed flat universe [See Table 2]. We repeat the same exercise (reconstruction of Ω_k^0) in open and closed universe also. We observe that the reconstructed region completely encloses the presumed value of Ω_k^0 within the 1σ confidence level and remains constant with respect to the redshift. This shows consistency with the assumption of homogeneity of the universe and also concordance with the FLRW metric.

4.2 Method II

In this method, we use another approach to constrain the curvature of the universe which is based on the FLRW metric. TOG (1984) [59], Gott, Park & Lee (1989) [28], Fukugita et. al. (1992) [63] and Lee & Park(1994) [67] construct the framework where statistical properties of gravitational lenses can be used to constrain the deceleration parameter and the cosmological constant.

Park & Gott [PG] (1997) [61] and Helbig [60] first proposed the use of statistical properties of gravitational lenses as a cosmological test for the curvature of universe. PG used a dataset of 20 multiple-image lens systems [76, 77] and observed a strong negative correlation between the image separation and the source redshift. In order to search for the possible cause of this, Yoon & Park (1996) [78] tried to study the effect of the evolution of lensing galaxies, clusters and curvature of the universe on the image separation of lenses. However, Helbig [60] showed that in an inhomogeneous universe a negative correlation is expected regardless of the value of cosmic curvature and argued that PG had used an inhomogeneous sample of gravitational lenses from the literature. Khare (2001)[68] further extended this analysis by using a dataset of 39 QSO lens systems of CfA/ Arizona Space Telescope Lens Survey [CASTLES][79] and found no significant correlation (weak negative correlation). However recently, Xia et.al. [80] use the 118 galactic-scale strong gravitational lensing (SGL) systems to constrain the cosmic curvature and find it to be close to zero.

In this work, we use the image separation data of lensed quasars in two different ways. First we divide the data into different redshift bins. After that we apply the GP smoothing technique to understand the variation of $\Delta\theta$ w.r.t. source redshift. Second, we apply different statistical test on the complete data of 44 points of image separation in order to explain the possible correlation between the two variables ($\Delta\theta$ and z_S).

The brief summary of the result is as follows:

- In Fig. 5, the best-fit line which represents the normalized mean image separation shows an inclination towards a close universe. However, within the 3σ region it also incorporates a flat universe. Though this inclination of best-fit line towards a closed universe can't be directly taken as the deviation from a flat universe, it does motivate us to study some of the proposed non-flat dark energy models [5–8]. Han & Park (2014) [62] have shown that the mean image separation in the presence of a direct or indirect angular selection bias or from a selection bias due to the limiting magnitude on the lens, manifests itself as an inclination towards the positive side with increasing source redshift. Hence, it is possible that the deviation of the reconstructed curve in Fig.5 is a result of the various selection criteria in the formation of the dataset which can give rise to a definite bias in our result.

- Though the different bin sizes result in a difference in the number of data points, the overall trend remains the same and with a small bin-size we obtain comparatively tight bands. From this we can argue that in future, with the availability of more observations, the bin-sizes can be reduced and more precise constraints can be obtained on cosmic curvature using the same method. We also believe that this test could serve as a new window to study the cosmic curvature in a model independent way.

- In order to quantify the correlation, if any, we apply Pearson product-moment correlation, Spearman rank correlation test and Kendall rank correlation test on the image separation versus redshift dataset (as shown in Table 1). Contrary to the previous work [61, 68], we observe a weak positive correlation between the variables. This result is further consistent with reconstructed curve of the normalized mean image separation vs source redshift by using GP (See Fig 5).

Finally, we can conclude that Method I probes the assumptions of a FLRW universe and homogeneity of the universe and we observe that it confirms both the assumptions. We also find $\Omega_k^0 = 0.025 \pm 0.57$ (with $H_0 = 73.24 \pm 1.74$ Km/sec/Mpc) for a presumed flat universe. Moreover, Method II, the indirect test based on the image separation of gravitational lenses, shows the consistency with a flat universe within the 3σ confidence region (see Fig.5). However the best fit line shows deviation from the flat universe prediction which could be due to selection effects as explained above. Thus we can say that both the methods used in this work jointly indicate a homogeneous but marginally closed universe. However, a flat universe can be incorporated at 3σ confidence level. In the near future with the availability of large datasets from various surveys, we would be able to put some very tight bounds on the cosmic curvature using the same model independent and geometric tests.

Acknowledgments

Authors are thankful to the reviewer for extremely useful comments and to Myeong- Gu Park, Phillip Helbig, Tong Jie Zhang & Yu Hai for useful discussions. A.R. acknowledges support under a CSIR-JRF scheme (Govt. of India, FNo. 09/045(1345/2014-EMR-I)) and also thanks IRC, University of Delhi for providing research facilities. A.M. thanks Research Council, University of Delhi, Delhi, India for providing support under R & D scheme 2015 -16.

References

- [1] E. Komatsu et. al., *WMAP collaboration, Seven-Year Wilkinson Microwave Anisotropy Probe (WMAP) Observations: Cosmological Interpretation*, ApJS 192 (2011) 18. [arXiv:1001.4538]
- [2] P.A.R. Ade et al., *Planck Collaboration, Planck 2015 results. XIII. Cosmological parameters*, A&A 594 (2016) A13. [arXiv:1502.01589]
- [3] D.J. Shaw & J.D. Barrow, *A Testable Solution of the Cosmological Constant and Coincidence Problems*, PRD 83 (2011) 043518. [arXiv:1010.4262]
- [4] C. Clarkson, B.A. Bassett & T.H. Lu, *A general test of the Copernican Principle*, PRL 101 (2008) 011301. [arXiv:0712.3457]
- [5] Pavlov et.al, *Nonflat time-variable dark energy cosmology*, PRD 88 (2013) 123513. [arXiv:1307.7399]
- [6] O. Farooq, D. Mania & B. Ratra, *Observational constraints on non-flat dynamical dark energy cosmological models*, [arXiv:1308.0834]
- [7] Y. Chen et.al., *Constraints on non-flat cosmologies with massive neutrinos after Planck 2015*, ApJ 829 (2016) 61. [arXiv:1603.07115]
- [8] O. Farooq et.al., *Hubble parameter measurement constraints on the redshift of the deceleration-acceleration transition, dynamical dark energy, and space curvature.*, ApJ 835 (2017) 26. [arXiv:1607.03537]
- [9] C. Clarkson, M. Cortes, & B. Bassett, *Dynamical Dark energy or simply cosmic curvature*, JCAP 07 (2007) 08. [arXiv:0702670]
- [10] F.X. Dupe, A. Rassat, J.L. Starck & M. J. Fadili, *Measuring the Integrated Sachs Wolfe Effect*, A&A 534 (2011) A51. [arXiv:1010.2192]
- [11] G. Bernstein, *Metric Tests for Curvature from Weak Lensing and Baryon Acoustic Oscillations*, ApJ 637 (2006) 598. [arXiv:0503276]
- [12] S. Rasanen, K. Bolejko & A. Finoguenov, *New Test of the Friedmann-Lematre-Robertson-Walker Metric Using the Distance Sum Rule*, PRD 115 (2015) 101301. [arXiv:1412.4976]
- [13] J.D. Barrow & F. J. Tipler, *The Anthropic Cosmological Principle*, ISBN: 978-0192821478, Oxford publication.
- [14] T. Buchert & M. Carfora, *On the curvature of the present day universe*, Class. Quant. Grav. 25 (2008) 195001. [arXiv:0803.1401]
- [15] H. Skarke, *Inhomogeneity implies Accelerated Expansion*, PRD 89 (2014) 043506. [arXiv:1310.1028]
- [16] M. Kleban & M. Schillo, *Spatial Curvature Falsifies Eternal Inflation*, JCAP 06 (2012) 029. [arXiv:1202.5037]
- [17] A.H. Guth & Y. Nomura, *What can the observation of nonzero curvature tell us?*, PRD 86 (2012) 023534. [arXiv:1203.6876]
- [18] A. H. Guth, D.I. Kaiser & Y. Nomura, *Inflationary Paradigm after Planck 2013*, PLB 733 (2014) 112. [arXiv:1312.7619]
- [19] J.R. Gott III, *Creation of open universes from de Sitter space*, Nature 295 (1982) 304.
- [20] B. Ratra et.al., *CMB Anisotropy in COBE-DMR-Normalized Open CDM Cosmogony*, ApJ 481 (1997) 22. [arXiv:astro-ph/9512148]
- [21] B. Ratra & P. J. E. Peebles, *Inflation in an open universe*, PRD 52 (1995) 1837.
- [22] M. Kamionkowski et.al., *CBR Anisotropy in an Open Inflation, CDM Cosmogony*, ApJ 444 (1995) L65. [arXiv:astro-ph/9406069].
- [23] M. Bucher, A.S. Goldhaber & N. Turok, *An Open universe from Inflation*, PRD 52 (1995) 3314. [arXiv:hep-ph/9411206].

- [24] D.H. Lyth & A. Woszczyna, *Large scale perturbations in Open universe*. PRD 52 (1995) 3338. [arXiv:astro-ph/9501044]
- [25] K. Yamamoto, M. Sasaki & T. Tanaka, *Large Angle CMB Anisotropy in an Open universe in the One-Bubble Inflationary Scenario*, ApJ 455 (1995) 412. [arXiv:astro-ph/9501109]
- [26] K.M.Gorski et.al. *COBE DMR-normalized open inflation cold dark matter cosmogony* , ApJ 444 (1995) 2. [arXiv:astro-ph/9502034]
- [27] R.F.L. Holanda, J.F. Jesus & M.A. Dantas, *Age of old objects constraints on cosmic opacity*. [arXiv:1605.01342]
- [28] J.R. Gott, M.G Park & H.M. Lee, *Setting limits on q_0 from gravitational lensing*, ApJ 338 (1989) 12.
- [29] N. Inada et.al, *The Sloan Digital Sky Survey Quasar Lens Search. V. Final Catalog from the Seventh Data Release*, Astron.J. 143 (2012) 119. [arXiv:1203.1087]
- [30] D. Sapone, E. Majerotto & S Nesseris, *Curvature vs Distance: testing the FLRW cosmology*, PRD 90 (2014) 023012. [arXiv:1402.2236]
- [31] E. Mortsell & J. Jonsson, *A model independent measure of the large scale curvature of the universe*. [arXiv:1102.4485]
- [32] Y.L. Li et. al., *Model-Independent Determination of Curvature Parameter Using $H(z)$ and $D_A(z)$ Data Pairs from BAO Measurements*, ApJ 789 (2014) 15. [arXiv:1404.0773]
- [33] R.G. Cai, Z.K. Guo & T. Yang, *Null test of the cosmic curvature using $H(z)$ and supernovae data*, PRD 93 (2016) 043517. [arXiv:1509.06283]
- [34] J.J Wei & X.F. Wu, *An Improved Method to Measure the Cosmic Curvature* (2016). [arXiv:1611.00904]
- [35] Z. Li, G.J. Wang, K. Liao & Z.H. Zhu, *Model-independent estimations for the curvature from standard candles and clocks*. [arXiv:1611.00359]
- [36] B. L'Huillier & A. Shafieloo, *Model-independent test of the FLRW metric, the flatness of the universe, and non-local measurement of H_0* . [arXiv:1606.06832]
- [37] R.G. Abraham et al., *The Gemini Deep Deep Survey. I. Introduction to the Survey, Catalogs, and Composite Spectra*, Astron.J. 127 (2004) 24. [arXiv:0402436]
P.J. McCarthy et al., *Evolved Galaxies at $z > 1.5$ from the Gemini Deep Deep Survey: The Formation Epoch of Massive Stellar Systems*, ApJ 614 (2004) 09. [arXiv:0408367]
- [38] T. Treu et. al., *A NICMOS search for high redshift elliptical galaxy candidates*, ApJ 524 (1999) 27. [arXiv:9907178]
T. Treu et. al., *The properties of field elliptical galaxies at intermediate redshift. I: empirical scaling laws*, MNRAS 308 (1999) 1037. [arXiv:9904327]
T. Treu et. al., *The properties of field elliptical galaxies at intermediate redshift. 2. photometry and spectroscopy of an hst selected sample*, MNRAS 326 (2001) 221. [arXiv:0104177].
- [39] R. Jimenez et. al., *Synthetic stellar populations: Single stellar populations, stellar interior models and primordial proto-galaxies*, MNRAS 349 (2004) 240. [arXiv:0402271]
- [40] J. Simon, L. Verde & J. Jimenez, *Constraints on the redshift dependence of the dark energy potential*, PRD 71 (2005) 123001. [arXiv:0412269]
- [41] J.J. Wei et.al., *The age redshift relationship of old passive galaxies.*, Astron.J. 150 (2015) 35. [arXiv:1505.07671]
- [42] M.A. Dantas et. al., *Current lookback time-redshift bounds on dark energy*, PLB 679 (2009) 423. [arXiv:0901.2327]
- [43] M.A. Dantas et al., *Time and distance constraints on accelerating cosmological models* , PLB 699 (2011) 239. [arXiv:1010.0995]

- [44] L. Samushia et.al, *Constraints on dark energy from the lookback time versus redshift test*, PLB 693 (2010) 509. [arXiv:0906.2734]
- [45] C. Blake et.al., *The WiggleZ Dark Energy Survey: the growth rate of cosmic structure since redshift $z=0.9$* , MNRAS 425 (2012) 405. [arXiv:1104.2948]
- [46] S. Alam et.al, *The clustering of galaxies in the completed SDSS-III Baryon Oscillation Spectroscopic Survey: cosmological analysis of the DR12 galaxy sample* [(arXiv:1607.03155)]
- [47] M. Moresco, *Raising the bar: new constraints on the Hubble parameter with cosmic chronometers at $z \sim 2$* , MNRAS 450 (2015) 16. [arXiv:1503.01116]
- [48] T. Delubac et.al. *Baryon Acoustic Oscillations in the Ly α forest of BOSS DR11 quasars*, A&A 574 (2015) A59. [arXiv:1404.1801]
- [49] A. Font-Ribera, *Quasar-Lyman Forest Cross-Correlation from BOSS DR11 : Baryon Acoustic Oscillations*, JCAP 05 (2014) 27. [arXiv:1311.1767]
- [50] Y. Chen & B. Ratra, *Median Statistics and the Hubble Constant*, Publ. Astron. Soc. Pacific 123 (2011) 907. [arXiv:1105.5206]
- [51] J.L. Sievers et al., *The Atacama Cosmology Telescope: Cosmological parameters from three seasons of data*, JCAP 10 (2013) 060. [arXiv:1301.0824]
- [52] G. Hinshaw et al. *Nine-Year Wilkinson Microwave Anisotropy Probe (WMAP) Observations: Cosmological Parameter Results*, ApJS (2013) 208 19 [arXiv:1212.5226]
- [53] E. Aubourg et al. *Cosmological implications of baryon acoustic oscillation (BAO) measurements*, PRD 92 (2015) 123516. [arXiv:1411.1074]
- [54] P.A.R. Ade et al. *Planck 2015 results. XIII. Cosmological parameters*, A&A 594 (2016) A13. [arXiv:1502.01589]
- [55] Y. Chen, S. Kumar & B.Ratra, *Determining the Hubble constant from Hubble parameter measurements*, ApJ 835 (2017) 86. [arXiv:1606.07316]
- [56] A.G. Riess et. al., *A 2.4% Determination of the Local Value of the Hubble Constant*, ApJ 826 (2016) 56. [arXiv:1604.01424]
- [57] C. E. Rasmussen & C.K.I. Williams, *Gaussian Processes for Machine Learning*, ISBN 026218253X.c MIT Press (2006). www.GaussianProcess.org/gpml
- [58] M. Seikel, C. Clarkson & M. Smith, *Reconstruction of dark energy and expansion dynamics using Gaussian processes*, JCAP 06 (2012) 036. [arXiv:1204.2832].
- [59] E.L. Turner, J.P. Ostriker & J.R. Gott, *The statistics of gravitational lenses - The distributions of image angular separations and lens redshifts*, ApJ 284 (1984) 01.
- [60] P. Helbig, *The $\Delta\theta - z_s$ relation for gravitational lenses as a cosmological test*, MNRAS 298 (1998) 02. [arXiv:9804104]
- [61] M.G. Park & J.R Gott, *Curvature of the universe and observed gravitational lens image separation vs. redshift*, ApJ 489 (1997) 476. [arXiv:09702173]
- [62] D.H. Han & M.G. Park, *Constraining cosmology with image separation statistics for gravitationally-lensed quasars in the Sloan Digital Sky Survey*, Jour. Korean Astron. Soc. 65 (2014) 827.
- [63] M. Fukugita, T.Futamase, M. Kasai & E.L. Turner, *Statistical properties of gravitational lenses with a nonzero cosmological constant*, ApJ 393 (1992) 03.
- [64] A. Dev, D. Jain & S. Mahajan, *Dark Energy and the statistical study of the observed image separations of the multiply imaged systems in the class statistical sample*, IJMPD 13 (2004) 06. [arXiv:0307441]
- [65] R. Kayser, P. Helbig & T. Schramm, *A General and practical method for calculating cosmological distances*, ApJ 318 (1997) 680. [arXiv:9603028]

- [66] C. Keeton, *A Catalog of Mass Models for Gravitational Lensing*, [arXiv:0102341]
- [67] H.A. Lee, & M.G. Park, *Statistical properties of gravitational lanes in cosmological models with cosmological constant*, Jour. Korean Astron. Soc. 27 (1994) 103.
- [68] P. Khare, *Angular separations of lensed quasar images*, ApJ 550 (2001) 153.
- [69] W.H. Press, S.A. Teukolsky, W.T. Vetterling & Brian P. Flannery, *Numerical Recipes in C* [ISBN-13: 978-0521431088], Cambridge University Press.
- [70] T. Buchert, A.A. Coley, H. Kleinert, B.F. Roukema, D.L. Wiltshire, *Observational challenges for the standard FLRW model*, IJMPD 25 (2016) 244 [arXiv:1512.03313]
- [71] D. L. Wiltshire, *Average observational quantities in the timescape cosmology*, PRD 80 (2009) 123512. [arXiv:0909.0749]
- [72] C. Boehm & S. Rasanen, *Violation of the FRW consistency condition as a signature of backreaction*, JCAP 09 (2013) 003. [arXiv:1305.7139]
- [73] A. Shafieloo & C. Clarkson, *Model independent tests of the standard cosmological model*, PRD 81 (2010) 083537. [arXiv:0911.4858]
- [74] H. Yu & F.Y. Wang, *New Model independent method to test the Curvature of the universe*, ApJ 828 (2016) 85. [arXiv:1605.02483]
- [75] A. Avgoustidis, L. Verde & R. Jimenez, *Consistency among distance measurements: transparency, BAO scale and accelerated expansion*, JCAP 09 (2009) 06. [arXiv:0902.2006]
- [76] J. Surdej & G. Soucail, in *Gravitational Lenses in the universe*, ed. by J. Surdej, D. Fraipont-Caro, E. Gosset, S. Refsdal, & M. Remy, Liege, Universitede Liege 205 (1994).
- [77] C.R. Keeton & C.S. Kochanek, *Astrophysical Applications of Gravitational Lensing*, I.A.U. Symp. No. 173 (1996).
- [78] S.Y. Yoon & M.G. Park, *Statistics of Gravitational Lensing by a Galaxy in Cluster or in Field*, Jour. Korean Astron. Soc. 29 (1996) 119.
- [79] CASTLES; CfA/ Arizona space telescope lens survey; <https://www.cfa.harvard.edu/castles/>
- [80] J.Q. Xia et. al., *Revisiting Constraints on Statistic Property of Strong Gravitational Lens System and Curvature of universe Model-independent*. [arXiv:1611.04731]
- [81] C. Zhang et al., *Four New Observational $H(z)$ Data From Luminous Red Galaxies of Sloan Digital Sky Survey Data Release Seven*, RAA 14 (2014) A10. [arXiv:1207.4541]
- [82] M. Moresco et al., *Improved constraints on the expansion rate of the universe up to $z \sim 1.1$ from the spectroscopic evolution of cosmic chronometers*, JCAP 08 (2012) 006. [arXiv:1201.3609]
- [83] M. Moresco et al., *A 6% measurement of the Hubble parameter at $z \sim 0.45$: direct evidence of the epoch of cosmic re-acceleration*, JCAP 05 (2016) 14. [arXiv:1601.01701]
- [84] D. Stern et al., *Cosmic Chronometers: Constraining the Equation of State of Dark Energy. I: $H(z)$ Measurements*, JCAP 02 (2010) 08. [arXiv:0907.3149]

Sr.No	z	H(z)	σ_H	Reference	Method and data used	Comment
1	0.070	69	19.6	[81]	SDSS DR7	A
2	0.090	69	12	[40]	GDDS+RG	R^a
3	0.120	68.6	26.2	[81]	SDSS DR7	A
4	0.170	83	8	[40]	GDDS+RG+SPEED	R^a
5	0.179	75	4	[82]	D4000 GSA	A
6	0.199	75	5	[82]	D4000 GSA	A
7	0.200	72.9	29.6	[81]	SDSS DR7	A
8	0.270	77	14	[40]	GDDS+RG+SPEED	R^a
9	0.280	88.8	36.6	[81]	SDSS DR7	A
10	0.352	83	14	[82]	D4000 GSA	A
11	0.380	81.5	1.9	[46]	BAO	A
12	0.3802	83	14	[83]	BOSS DR-9	A
13	0.400	95	17	[40]	GDDS+RG+SPEED	R^a
14	0.4004	77	10.2	[83]	BOSS DR-9	A
15	0.4247	87.1	11.2	[83]	BOSS DR-9	A
16	0.440	82.6	7.8	[45]	BAO	A
17	0.4447	92.8	12.9	[83]	BOSS DR-9	A
18	0.4783	80.9	9	[83]	BOSS DR-9	A
19	0.480	97	62	[84]	SDSS LRDs + KC	A
20	0.510	90.5	1.9	[46]	BAO	A
21	0.593	104	13	[82]	D4000 GSA	A
22	0.600	87.9	6.1	[45]	BAO	A
23	0.610	97.3	2.1	[46]	BAO	A
24	0.680	92	8	[82]	D4000 GSA	A
25	0.730	97.3	7.0	[45]	BAO	A
26	0.781	105	12	[82]	D4000 GSA	A
27	0.875	125	17	[82]	D4000 GSA	A
28	0.880	90	40	[84]	SDSS LRDs + KC	A
29	0.900	117	23	[40]	GDDS+RG+SPEED	R^a
30	1.037	154	20	[82]	D4000 GSA	A
31	1.300	168	17	[40]	GDDS+RG+SPEED	R^a
32	1.363	160	33.6	[82]	D4000 GSA	A
33	1.430	177	18	[40]	GDDS+RG+SPEED	R^a
34	1.530	140	14	[40]	GDDS+RG+SPEED	R^a
35	1.750	202	40	[40]	GDDS+RG+SPEED	R^a
36	1.965	186.5	50.4	[47]	D4000 GSA	R^b
37	2.340	222	7	[48]	BOSS DR11	R^b
38	2.360	226	8	[49]	BOSS DR11	R^b

Table 3: 38 Hubble data points. "A" indicates the Hubble points accepted for calculation of Ω_k^0 . " R^a " shows the Hubble points removed from calculation as these points are used to calculate transverse comoving distance, " R^b " represents the points removed to avoid extrapolation as transverse comoving distance lies in redshift range $0 < z < 1.84$